Circuit modeling and simulation of the ESD generator for various tested equipment according to the IEC 61000-4-2

GEORGIOS FOTIS, VASILIKI VITA

Department of Electrical and Electronics Engineering Educators
ASPETE - School of Pedagogical and Technological Education
N. Heraklion, 14121, GREECE

Abstract: - The existing IEC Standard for Electrostatic Discharge (ESD) contains a general and simplified circuit for the generator that produces ESD discharges, without entering into details. The present work tries to fill this gap and proposes a circuit which will generate the ESD current in the limits that the current Standard defines. Two circuit models are examined through simulations with SPICE software, with the one to be the most suitable. This circuit model is also examined for various loads that simulate the Equipment under Test (EUT) and useful conclusions derive up to what type and size of equipment can be safely tested by ESD generators so that the test results are reliable.

Key-Words: - Circuit modeling, electrostatic discharge, ESD generator, Equipment Under Test (EUT), IEC 61000-4-2, SPICE Software.

Received: July 27, 2021. Revised: July 12, 2022. Accepted: August 18, 2022. Published: September 1, 2022.

1 Introduction

The abrupt transfer of charge between objects at various electrostatic potentials is known as Electrostatic Discharge (ESD) [1]. Triboelectric charging is the process of creating electrostatic charge through the contact and separation of materials. It entails the transfer of electrons among various materials. ESD is clearly a transient overvoltage pulse with a sharp rising edge, a large current amplitude, and little energy. ESD has a great impact on electronic equipment, which may be destroyed if it not shielded and designed properly [2].

The majority of ESD procedures are referred to the most recent version of the IEC Standard 61000-4-2 [3]. The purpose of this Standard is to create a consistent and repeatable framework for assessing how electrical and electronic equipment performs when exposed to electrostatic discharges. The Human Body Model (HBM), which simulates the electrostatic discharge of the human body on electrical or electronic equipment, is the starting point of this Standard. The study of the ESD current waveforms has involved an in depth investigation. The amplitudes and rise times of ESD current waveforms have been demonstrated to change with charging voltages, approach speeds, electrode types, and humidity [4-7].

There have been various publications which propose an enhanced circuit for ESD generators [8-12]. A modified ESD generator and an equation for the reference waveform have both been proposed in [9]. The redesigned ESD generator has a reference waveform that is quite similar to the one specified by the IEC Standard. Another study uses SPICE software to the accepted HBM, which is broken down into 11 basic building pieces [10]. The factors that control the discharge current waveforms of ESD generators are clarified in [11], which also proposes an analogous circuit model based on the design and dimensions of the ESD generator. Two precise models for electrostatic discharge generators are put out in [12] and allow for the reproduction of the discharge current in the contact mode while taking the load effect into account.

There have also been studies of finding an accurate equation that can describe the ESD current's waveform as it is described in the IEC Standard [3]. The ESD current can be approximated using an equation separate from the circuits for the ESD generators. The ESD generator can be correctly described using this equation in modeling software. These studies enable a Genetic Algorithm by whom the ESD current's equation parameters are optimized [13-15]. Also, there have been previous works that describe the procedure where the ESD circuit can

derive from this accurate equation using the Prony's method [16].

Another crucial issue in the ESD study is the electromagnetic field that the ESD generators produce, which may affect in various ways the equipment they test each time affecting the test result [17-19]. This is something that is still studied and it is mentioned without certain directions in the current IEC Standard for ESD [3].

In this paper a new circuit for the ESD generator is proposed according to the IEC Standard. After simulations in the SPICE program the waveform of the ESD current that derives from the proposed circuit it is found that is in the specified limits by the Standard.

2 The IEC 61000-4-2

The current that the ESD generators have to produce is depicted in Figure 1, according to the IEC 61000-4-2 [3]. There are four parameters whose values have to be in specific limits: the rise time (t_r), the peak discharge current (I_p), the current at 30 ns (I_{30}) and the current at 60 ns (I_{60}). These two current values I_{30} and I_{60} are determined for a period of 30 ns and 60 ns, respectively, commencing at the time point when the current equals 10% of the peak current, as shown in Figure 1. These parameters' limits, as given in Table 1, are valid only for contact discharges.

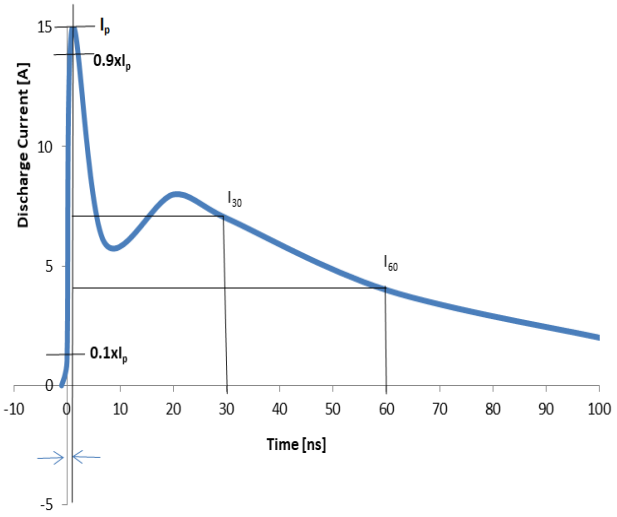

Figure 1 Typical waveform of the output current of the ESD gun for contact discharges.

A simplified diagram of the test generator is presented in Figure 2 and it consists, in its main parts: the charging resistor R_c, the energy-storage capacitor C_s, the distributed capacitance C_d, the discharge resistor R_d, the voltage indicator, the discharge switch, the charge switch, the interchangeable tips of the discharge electrode, the discharge return cable and the power supply unit.

Table 1 Waveform parameters of the ESD current for contact discharges according to the IEC 61000-4-2.

Indicated Voltage [kV]	I_{max} [A] (±15%)	t_r [ns] (±25%)	I_{30} [A] (±30%)	I_{60} [A] (±30%)
2	7.5	0.8	4	2
4	15	0.8	8	4
6	22.5	0.8	12	6
8	30	0.8	16	8

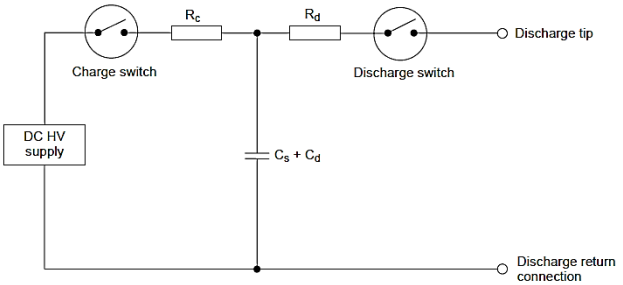

Figure 2 A simplified diagram of the ESD generator according to the IEC 61000-4-2.

The generator must comply with the requirements given the IEC 61000-4-2. Therefore, neither the diagram in Figure 2, nor the element values are specified in detail. This significant gap of the IEC Standard need to be investigates and this is the main objective of this work.

3 ESD circuit for SPICE simulations

For the needs of SPICE simulation it is necessary to find an equivalent discharge circuit for the ESD generator. Next, the individual elements of which the electrostatic discharge generator was composed during the SPICE simulation are presented. According to the Standard [3] the ESD gun and the Equipment under Test (EUT) are connected via the electrode and the 2m long ground wire permitting the current return. The cable is twisted and covered with insulating material designed to have reduced resistance and inductance. Its resistance has a very small value and can be neglected compared to the resistance of the discharge circuit and the resistance of the load.

3.1 Calculation of inductive elements

The value of the inductance of the ground wire mainly affects the response of the circuit. For a cable of length l and permittivity μ, with width w and

density t, the following formula is proposed for the inductance L_r in μH [8], [20]:

$$L_r = 0.002\left[\ln\left(\frac{2l}{w+t}\right) + 0.25049 + \frac{w+t}{3l} + \frac{\mu T(x)}{4}\right] \quad (1)$$

where T(x) is a frequency dependent function and in the case of high frequencies T(x)=0.

When designing a high frequency circuit there is difficulty in directly calculating the line inductance due to the non-uniform distribution of the charge on the line. In practice, the value of cable inductance is not affected by the type of cable cross-section. This is how a cable with a circular cross-section is studied. Since the wire is twisted, the angle is smooth, so the circular cross-section assumption facilitates the analysis. Considering a straight conductor of length l with a circular cross-section of radius a, the inductance L_s is given by the sum of the conductor's internal inductance L_{si} and the external inductance L_{se}:

$$L_s = L_{si} + L_{se} \quad (2)$$

$$L_{si} = \frac{\mu_0 l}{8\pi} \quad (3)$$

$$L_{se} = \frac{\mu_0}{2\pi}\left(l \ln\frac{l+\sqrt{\alpha^2+l^2}}{\alpha} - \sqrt{\alpha^2+l^2} + \alpha\right) \quad (4)$$

Equation (4) gives only the contribution of the magnetic field around the conductor and does not take into account the effect of other conductors. The test to check the immunity of equipment to electrostatic discharge currents is done inside an anechoic chamber and the equipment is placed on a conductive plate. Since the current flows on the conductive floor due to the magnetic field of the ground wire, the inductance cannot be neglected. Assuming that the distance between the floor and the center of the conductor is h with h<<l, the inductance L_{sm} of the ground wire is:

$$L_{sm} = L_{smi} + L_{sme} \quad (5)$$

$$L_{smi} = \frac{\mu_0 l}{8\pi} \quad (6)$$

$$L_{sme} = \frac{\mu_0 l}{2\pi}\ln\frac{2h-\alpha}{\alpha} \quad (7)$$

In the high frequency region, the magnetic field inside the conductor is zero and the inductances L_{si} and L_{smi} of equations (3) and (6) can be ignored.

3.2 The ground wire as a transmission line

In equation (5) it is assumed that the ground wire is placed above the conductive surface. Then a transmission line is created, which has the ground as its return path. Although the ground wire has an insulating sheath, which is some kind of dielectric, this layer is thin and does not affect the dielectric constant of the overall system. Therefore, the dielectric material can be neglected. Then, the transfer line satisfies (5) and (7). The characteristic resistance Z_m is given by the formula:

$$Z_m = 59.952 \ln\left(\frac{h}{\alpha} + \sqrt{\left(\frac{h}{\alpha}\right)^2 - 1}\right) [\Omega] \quad (8)$$

3.3 ESD generator's capacity

The construction of the gun as well as the capacitance C_m to earth can be represented by a metal sphere of radius a. If the distance of the center of the sphere from the floor is h, the capacitance can be calculated by considering its mirror image. The resulting expression is a series from which, ignoring terms of higher order, the following approximate formula is obtained:

$$C_m = \frac{8\pi\varepsilon_0\alpha h}{2h-\alpha} \quad (9)$$

3.4 Electrostatic discharge generator models for numerical analysis

The design of electronic automation is an ongoing development in electronics design, and methods for the numerical analysis of circuit response are already established. SPICE software for circuit analysis, is widely used to overcome many problems such as convergence [21]. In addition, models for integrated circuits are provided in SPICE. There are still models that describe various electromagnetic phenomena [22].

As can be seen from Figure 3, the construction of the equivalent circuit is complicated by the parasitic elements in the experimental space. For the existence of distributed capacitances, which are not included in the equivalent circuit, reference is made to the Standard but they are not shown in the circuit. If the allocated capacity does not exist, the initial maximum is not produced.

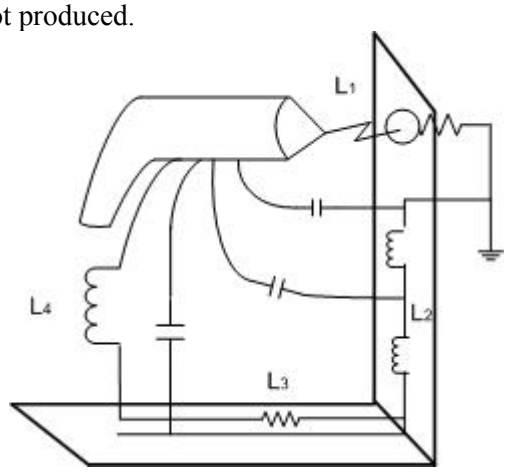

Figure 3 An ESD generator during discharges in a laboratory environment.

First, the values of the circuit constants are determined. Figure 4 shows the first circuit model used for the analysis. The circuit constants are interpreted as follows: R_1, R_2 and C_1 are defined by the Standard. For the determination of the remaining circuit elements, the parasitic elements should also be taken into account.

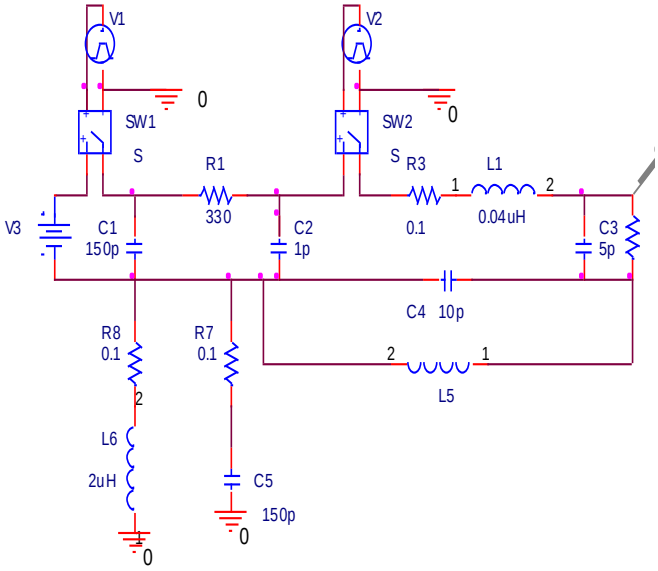

Figure 4 A proposed circuit model for the ESD generator (Circuit Model 1).

The value of the inductance should be determined independently since there are no specifications. The discharge gun electrode length is specified to be 50mm and the radius 6mm. Then, equation (4) is applied assuming that there is no magnetic field inside the conductor. Substituting l=50mm and α=6mm gives L_1=0.0193μH. In practice the discharge electrode and the discharge resistor are connected by a common wire. Taking into account the inductance of the cable, the value of L_1 is taken as 0.04μH. The surface inductance of the conductive target L_2 is sufficiently small and can be neglected compared to the inductance of the ground wire as long as it is 1m long and the surface is sufficiently large.

We assume that the ground wire has a diameter of 10mm. Substituting in (8) α=5 mm and h=6.84mm, Z_m=50Ω results. Subtracting the radius a of the conductor the ground wire is above the conductive surface by 1.84mm. This situation corresponds to a transmission line with a resistance of 50Ω, consistent with the real situation, if we also take into account the insulating surface. When the wire is shorter, but still considered a 50Ω transmission line, the inductance decreases more or less depending on the gap between them. Inside the conductor it is assumed that there is no magnetic field. Applying (7) and substituting h=6.84mm, l=1m it follows that L_3 of the conductive plate is equal to 0.11μH.

Equation (7) is not valid for calculating L_4 if the ground wire is more than 30cm from the metal plate on the target side. Applying (4) and substituting l=1m we get L_4=0.861μH. The inductances L_3 and L_4 differ by a factor greater than 8, even though they have the same lengths. This happens because the distances from the metal plate are different.

R_2 is the target resistance. The inductance L_5 of the ground wire is equal to the sum of L_2, L_3 and L_4, so L_5=1μH.

Equation (9) is applied to calculate the capacitance of the cable to earth. For α=3cm and h=20cm from the floor it follows that C_m=3.6pF. In practice the gun is held by a person who has a capacitance of C_5=150pF. Consequently it is not sufficient to replace the target capacitance by C_m alone. Thus C_4=10pF is set, including the capacitance of the human body.

Voltage V_3 is the supply to charge capacitor C_1. SW1 is the charge switch which is closed for the first 9ns and then opens, while SW2 is the discharge switch which is open for the first 10ns and then closes. Capacitor C_2 represents the stray capacitance around resistor R_1, which corresponds to the surface resistance. Capacitor C_3 simulates the parasitic capacitance around the sensor of the discharge current. L_6 is the inductance of the external ground wire connecting the supply to the gun. Finally, R_7 and R_8 are dummy resistors used to prevent oscillations.

In the equivalent circuit of Figure 5 the charge switch and the discharge switch are connected separately. They should be properly handled so that they are not both open or closed at the same time. To overcome this problem we proceed to redesign the switch as shown in Figure 5.

In Figure 6 which models the circuit of Figure 5, switch SW2 has been moved to the left of capacitor C_2 and resistor R_1. The circuit constants remain the same.

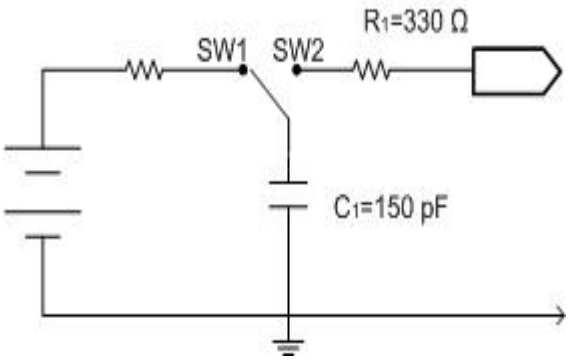

Figure 5 Circuit diagram of actual charger**.**

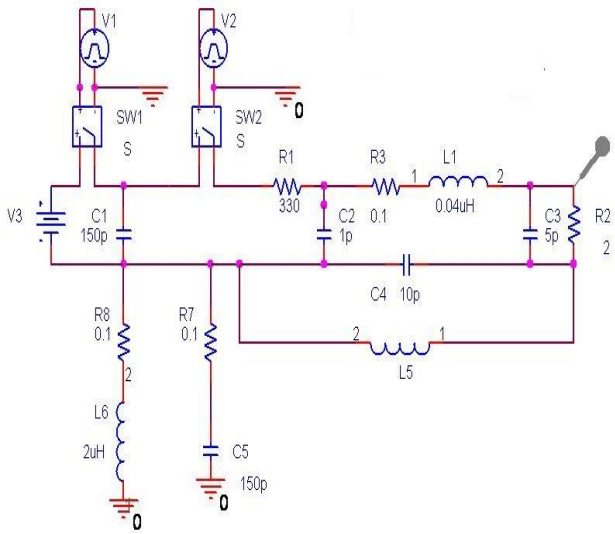

Figure 6 A proposed circuit model for the ESD generator (Circuit Model 2).

4 Current waveform analysis

4.1 Effect of ground wire on current waveforms

As demonstrated the ground wire inductance depends on the relative position of the ground wire to the ground plate. As previously mentioned it was assumed that the ground wire is parallel to the ground plate and L_5=1μH was calculated. When the ground wire is remote from the ground plate or no ground plate is present during the test then L_3=L_4 and therefore L_5=2μH. Figures 7 and 8 show the simulation results for L_5=1μH and L_5=2μH, for charging voltages of +1kV for both circuit models.

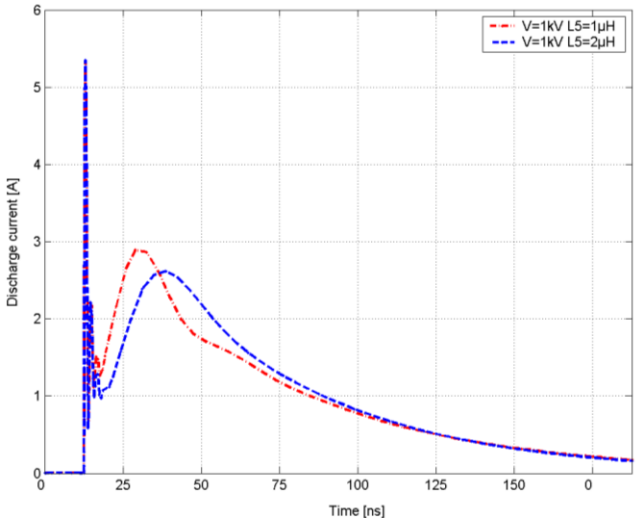

Figure 7 The produced ESD current of the Circuit Model 1.

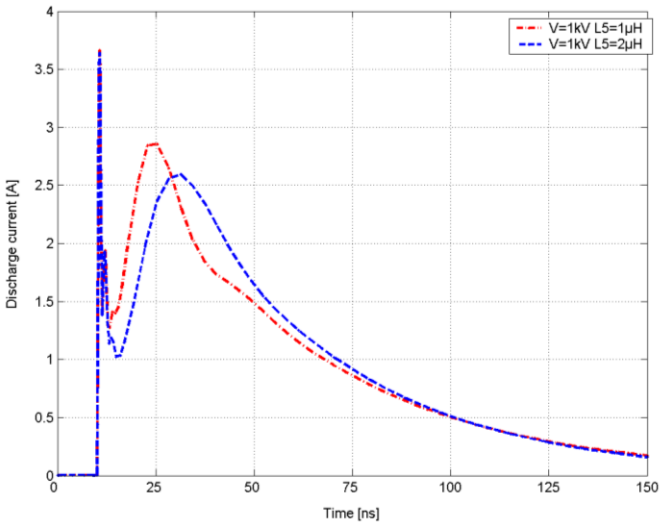

Figure 8 The produced ESD current of the Circuit Model 2.

Comparing Figures 7 and 8 we notice that the change in the switch mechanism affected I_{max} and in fact its value decreased. This is because the parasitic capacitance C_2 has changed from source to load due to the displacement of the discharge switch. For this reason it is important to determine the conditions under which the test is carried out so that all parameters are adjusted in such a way that the value of C_2 remains constant. It is also observed that the value of I_{max} obtained from model 1 is very high. This can be compensated by increasing the inductance L_1 which is affected by the length of the discharge electrode.

4.2 Comparison of the two electrostatic discharge generator circuits

With the help of the SPICE program, the two circuits of the electrostatic discharge generator (models 1 and 2) were implemented and a simulation was carried out for charging voltage values of +2kV and +4kV. Based on the results of the simulation it is possible to check the satisfaction of the criteria of the specifications by the parameters of the electrostatic discharge current as recorded in Table 1. In Table 2 the values of the discharge current parameters for model 1 and model 2 are presented for charging voltages of +2kV and +4kV. The discharge current for the two models and for the two charging voltages from the SPICE simulation are presented in Figures 9-12.

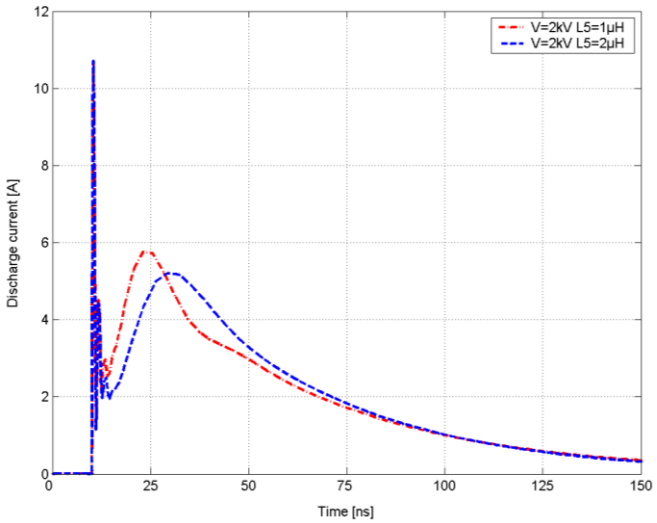

Figure 9 Response of the circuit model 1 for +2kV charging voltage.

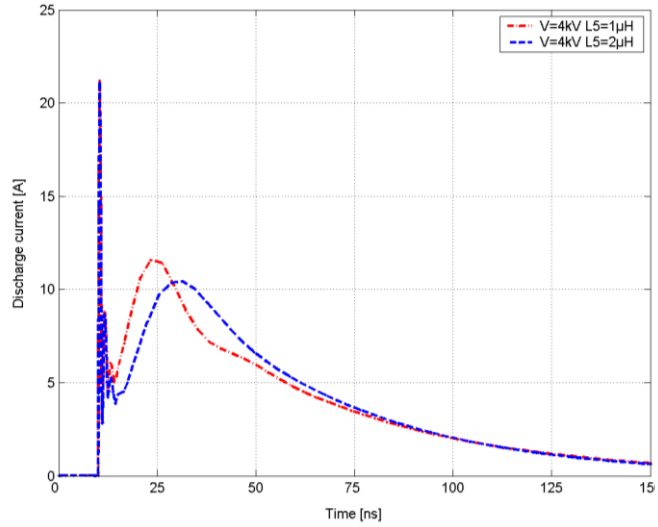

Figure 10 Response of the circuit model 1 for +4kV charging voltage.

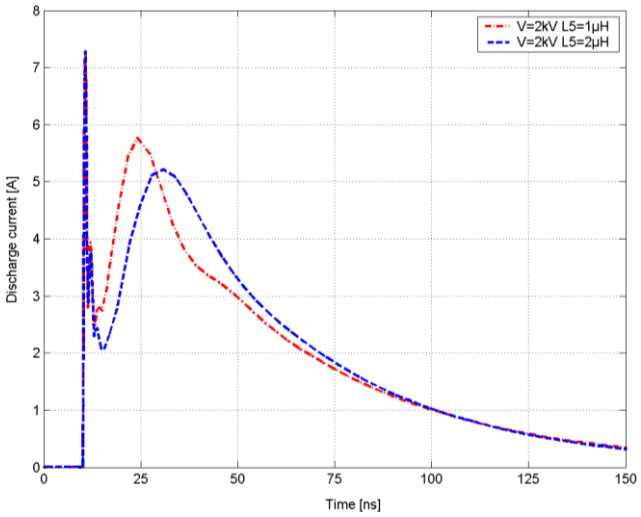

Figure 11 Response of the circuit model 2 for +2kV charging voltage.

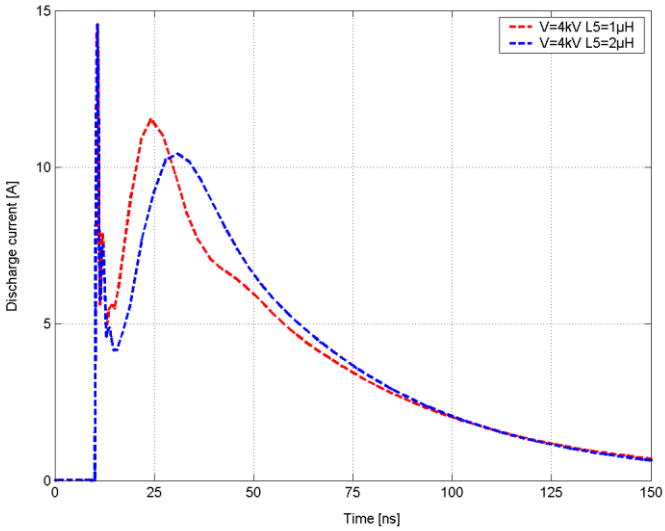

Figure 12 Response of the circuit model 2 for +4kV charging voltage.

Observing the values of Table 2 and comparing them with the limits of Table 1 we conclude that the specification limits met only for model 2, since the values of model 1 are out of the specified limits of the IEC Standard.

Table 2 Values of the discharge current parameters for model 1 and model 2.

Voltage [kV]		L_5 [μH]	I_{max} [A]	t_r [ns]	I_{30} [A]	I_{60} [A]
2	Model 1	1	10.72	0.261	3.49	1.91
		2	10.72	0.265	4.34	2.05
4		1	21.21	0.235	6.95	3.82
		2	21.11	0.237	8.71	4.10
2	Model 2	1	7.25	0.621	3.48	1.91
		2	7.28	0.635	4.37	2.05
4		1	14.49	0.637	6.96	3.81
		2	14.56	0.658	8.73	4.09

4.3 Testing the circuit for different EUT

For the circuit of model 2, which simulates the electrostatic discharge generator and for a value of L_5=1μH and a charging voltage of +2kV we have replaced the 2Ω target with resistive probes of a higher resistance value, with inductive as well as capacitive probes. The resulting waveforms are shown in the following Figures 13-15. In Table 3 the values of the critical parameters of the waveforms depicted in Figures 13-15 are listed so that it is possible to check whether their limits are satisfied.

From Figures 13-15 we notice that an increase in the resistance value of the EUT affects the waveform of the current and in fact as the value increases the waveform of the Standard ceases to be valid.

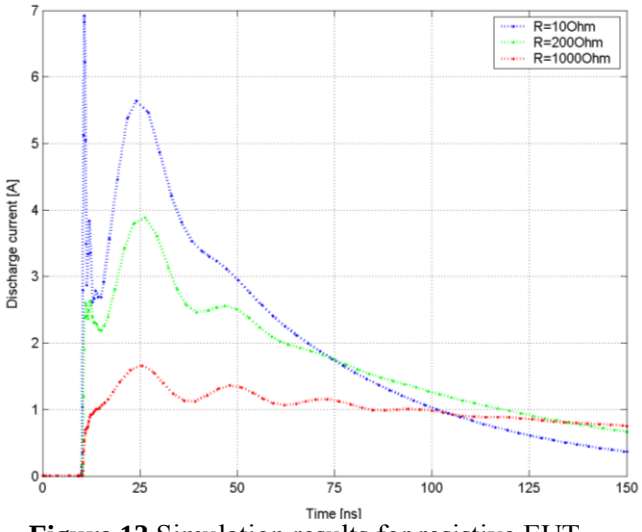

Figure 13 Simulation results for resistive EUT.

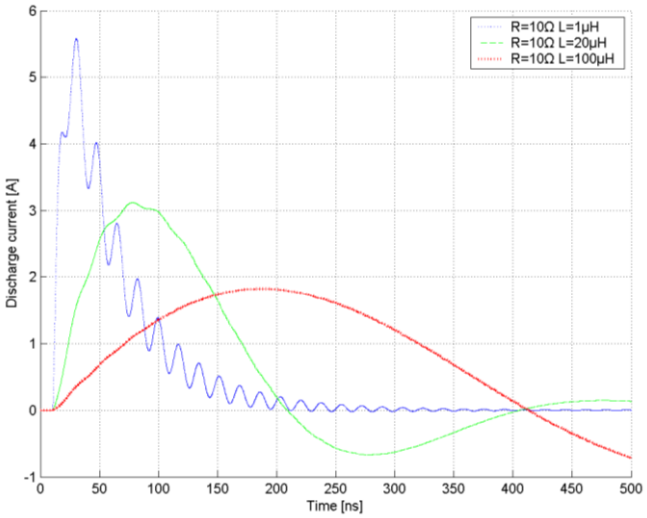

Figure 14 Simulation results for RL EUT.

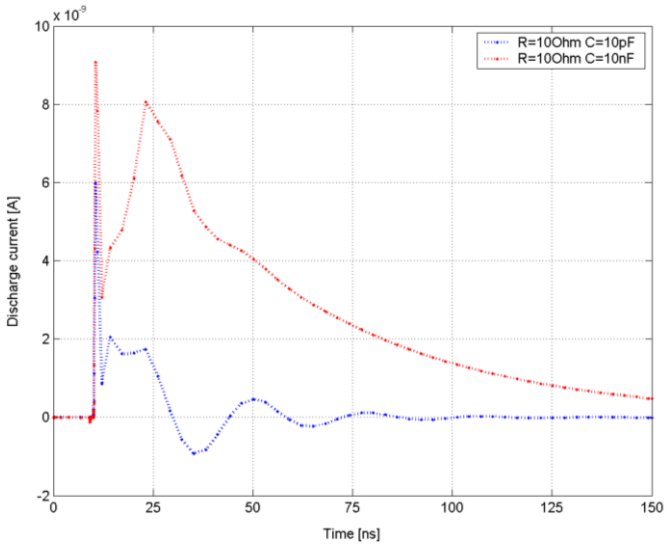

Figure 15 Simulation results for RC EUT.

Table 3 Current's parameter values for the circuit model 2 for various EUT types.

EUT Type	*R* [Ω]	*L* [μH]	C [pF]	I_{max} [A]	t_r [ns]	I_{30} [A]	I_{60} [A]
Ohmic (R)	10	0	0	6.9713	0.3883	3.3676	1.9145
	200	0	0	2.6068	0.5473	2.4678	1.8532
	1000	0	0	Current waveform out of limits			
Ohmic – Inductive (RL)	10	1	0	4.2086	0.7402	3.5315	2.5203
	10	20	0	Current waveform out of limits			
	10	100	0	Current waveform out of limits			
Ohmic – Capacitive (RC)	10	0	10	0.6E-09	0.3788	-5.9608E-11	-8.8058E-11
	100	0	10	9.0734E-09	0.3631	4.6569E-09	2.5975E-09

5. Conclusions

Electrostatic discharge is a potential danger for electronics and this is the reason that an electronic device must be tested by ESD generators before its massive production. The inner circuit of these generators must fulfill the specifications of the current Standard [3]. Although, this circuit is described in the Standard there is a gap on its specific constructional details and this is what this paper tried to fill.

A new circuit model for the ESD generator is proposed and simulations via SPICE software were conducted proving that the ESD current fulfills the Standard's specifications. Also, other simulations for various EUT, proved that an increase in the resistance value of the EUT affects the waveform of the current. This remark proves that a further investigation up to what type and size of equipment can be safely tested by ESD generators so that the test results are reliable must be made. The upcoming revision of the IEC Standard possibly should include these remarks.

References:

[1] Wang A., *Practical ESD Protection Design*, 1st Edition, Wiley-IEEE Press; 2021.

[2] Bafleur M.; Caignet F.; Nolhier N., *ESD Protection Methodologies: From Component to System*, 1st Edition, ISTE Press – Elsevier, 2017.

[3] *IEC 61000-4-2. Electromagnetic Compatibility (EMC)—Part 4-2: Electrostatic Discharge Immunity Test*, ed. 2.0. 2008. Available online: https://webstore.iec.ch/publication/4189.

[4] Pommerenke D., Aidam M.., ESD: waveform calculation, field and current of human and simulator ESD, *Journal of Electrostatics*, Vol. 38, No. 1-2, 1996, pp. 33-51.

[5] Bonisch S., Pommerenke D., Kalkner W., Broadband measurement of ESD risetimes to distinguish between different discharge mechanisms, *Journal of Electrostatics*, Vol. 56, No. 3,October 2002, pp. 363-383.

[6] Oikawa M., Kawamata K., Ishigami S., Minegishi S., Fujiwara O., Measurement of current distribution on electrode surface of spherical electrode caused by micro gap ESD, *IEEE 5th International Symposium on Electromagnetic Compatibility,* Beijing, China, 2017, pp. 1-4, doi: 10.1109/EMC-B.2017.8260482.

[7] Lin H., Sheng-zong H., You-liang W., Xiao-si L., Qi-zheng, J., Study on Electrostatic Discharge Damage and Defect Damage Failure Analysis Technology for Semiconductor Devices, *19th International Conference on Electronic Packaging Technology (ICEPT)*, Shanghai, China, 2018. doi: 10.1109/ICEPT.2018.8480420.

[8] Murota N., Determination of characteristics of the discharge current by the human charge model ESD Simulator, *Electronics and Communications in Japan*, Part 1, Vol. 80, No. 10, 1997. pp. 49-57.

[9] Wang, K., Pommerenke, D., Chundru, R., Doren, T.V., Drewniak, J.L., Shashindranath. A. Numerical modeling of electrostatic discharge generators, *IEEE Transactions on Electromagnetic Compatibility*, Vol. 45, No. 2, pp. 258–271.

[10] Amoruso V.; Helali M.; Lattarulo F. An improved model of man for ESD applications, *Journal of Electrostatics*, Vol. 49, o. 3-4, 2000, pp. 225–244.

[11] Fujiwara O., Tanaka H., Yamanaka Y., Equivalent circuit modelling of discharge

current injected in contact with an ESD-gun, *Electrical Engineering in Japan*, Vol. 149, 2004, pp. 8–14.
[12] Caniggia S., Maradei F., Circuital and numerical modelling of electrostatic discharge generators, *In Proceedings of the 14th IAS Annual Meeting, IEEE Industry Applications Conference*, Kowloon, Hong Kong, 8 August 2005; pp. 1119–1123.
[13] Vita V., Fotis G., Ekonomou L., An Optimization Algorithm for the Calculation of the Electrostatic Discharge Current Equations' Parameters, *WSEAS Transactions on Circuits and Systems*, Vol. 15, 2016, pp. 224-228.
[14] Vita V., Fotis G., Ekonomou L., Parameters' optimisation methods for the electrostatic discharge current equation, *International Journal of Energy*, Vol. 11, 2017, pp. 1-6.
[15] Fotis G., Ekonomou L., Parameters' Optimization of the Electrostatic Discharge Current, *International Journal on Power System Optimization*, Vol. 3, No 2, July – December 2011, pp. 75-80.
[16] Katsivelis P., Fotis G., Gonos I.F., Koussiouris T.G., Stathopoulos I.A., Electrostatic Discharge Current Linear Approach and Circuit Design Method. *Energies*, Vol. 3, 2010, pp. 1728-1740.
[17] Fotis G., Vita V., Ekonomou L. Machine Learning Techniques for the Prediction of the Magnetic and Electric Field of Electrostatic Discharges, *Electronics*. Vol. 11, No. 12, 2022. https://doi.org/10.3390/electronics11121858
[18] Fotis G., Ekonomou L., Maris T.I., Liatsis P., Development of an artificial neural network software tool for the assessment of the electromagnetic field radiating by electrostatic discharges, *IEE, Proceedings Science, Measurement & Technology*, Vol. 1, No 5, pp 261-269, 2007. https://doi.org/10.1049/iet-smt:20060137
[19] Ekonomou L., Fotis G., Maris T.I., Liatsis P., Estimation of the electromagnetic field radiating by electrostatic discharges using artificial neural networks. *Simulation Modelling Practice and Theory*, Vol. 15, No. 9, pp. 1089-1102, 2007. https://doi.org/10.1016/j.simpat.2007.07.003
[20] Greenhouse. H. M., Design of planar microelectronics inductors, *Transactions IEEE*, PHP-10, No.2, 1974, pp. 101-109.
[21] A. Vladimirescu, *The Spice Book*, Wiley (1994)
[22] Celozzi S., Felixiani M., Time-domain solution of field-excited multiconductor transmission line equation, *Transactions IEEE*, EMC-37, No3, 1995, pp. 421-432.

Contribution of Individual Authors to the Creation of a Scientific Article (Ghostwriting Policy)
The authors equally contributed in the present research, at all stages from the formulation of the problem to the final findings and solution.

Sources of Funding for Research Presented in a Scientific Article or Scientific Article Itself
No funding was received for conducting this study.

Conflict of Interest
The authors have no conflicts of interest to declare that are relevant to the content of this article.